

Hybrid Algorithm for Coordinated Design of PSSs and SVC

¹E. S. ALI, ²S. M. ABD ELAZIM

¹Electrical Engineering Department, Faculty of Engineering, Jazan University, KSA.

²Computer Science Department, Faculty of Computer Science and Information Technology, Jazan University, KSA.

Abstract- The evaluation of novel coordinated design of Power System Stabilizers (PSSs) and Static Var Compensator (SVC) in a multimachine system by statistical method is presented in this study. The coordinated design process of PSSs and SVC above a great range of loading is formed as an optimization task. The Bacterial Swarming Optimization (BSO), which couples synergistically the Bacterial Foraging (BF) with the Particle Swarm Optimization (PSO), is used to seek for optimum controllers elements. By reducing the suggested objective function, in which the speed variations among generators are engaged; stability investigation of the system is enhanced. To compare the ability of PSS and SVC, both are independently designed, and then in a coordinated way. Simultaneous setting of the BSO based on coordinated controller gives robust damping characteristics over a great range of operating conditions and wide disturbance compared with optimized PSS based on BSO (BSOPSS) and optimized SVC based on BSO (BSOSVC). Also, a statistical T test is done to assure the robustness of coordinated controller contra uncoordinated one.

Keywords: PSSs; SVC; Power System; Coordinated design; BSO; Statistical T test.

Received: April 26, 2021. Revised: June 20, 2022. Accepted: July 16, 2022. Published: September 2, 2022.

1. Introduction

The power transfer in an integrated power system is obliged by transient stability, voltage stability and small stability. These constraints define a full utilization of obtainable transmission corridors. Flexible AC Transmission System (FACTS) is the technology that supplies the necessary corrections of the transmission functionality to fully use the existing transmission facilities and then, reducing the gap among the stability and thermal limits [1].

Latterly, there has been an interest in the development and use of FACTS controllers in transmission systems [2 – 6]. These controllers use power electronics circuits to supply more flexibility to AC power systems. The most popular type of FACTS in terms of application is the SVC. This device is known to enhance system properties like stability limits, voltage regulation and var compensation, dynamic over and under voltage control, and damp system oscillations. The SVC is an electronic circuit that controls dynamically the flow of power through a variable admittance to the transmission system.

Eventually, various researchers have presented many techniques for planning SVC to improve the damping of oscillations of power systems and enhance systems stability. A robust control opinion in planning SVC controller to decay swing modes is presented in [7]. An adaptive network based fuzzy system for SVC is discussed in [8] to enhance the

alleviation of oscillations. A multi input, single output fuzzy neural network is introduced in [9] for voltage stability assessment of the power systems with SVC. A technique of determining the position of a SVC to improve the stability of power system is presented in [10]. A systematic approach for planning SVC controller, based on wide area signals, to enhance the damping of power system oscillations is suggested in [11]. Genetic Algorithm technique is employed for simultaneous tuning of a PSS and a SVC based controller in [12]. A state estimation task of power systems incorporating many FACTS circuit is developed in [13]. A fresh hybrid method for simulation of power systems equipped with SVC is addressed in [14]. The design of SVC with delayed input signal using a state space model based on Pade approximation method is introduced in [15]. Bacterial Foraging Optimization Algorithm (BFOA) for planning SVC to damp system oscillations for single machine infinite bus system and multimachine system is presented in [16]. Flower pollination algorithm is introduced in [17] for SVC design. An enforcement of probabilistic theory to the coordinated plan of PSSs and SVC is used in [18]. The implementation of the decentralized modal control style for pole placement in power system using FACTS circuits is displayed in [19]. The parameter setting of a PID controller for a FACTS based stabilizer using multi-objective evolutionary algorithm is discussed in [20]. A comprehensive evaluation of the effects of the PSS and FACT circuit

when independently applied and also via coordinated application is performed in [21].

Many optimization algorithms have been adopted to resolve a variety of engineering process in the past decade. GA has engaged the attention in the scope of controller parameter optimization. Although GA is satisfactory in detecting global or near global optimal result of the task; it requires a very long run time that may be various minutes or even many hours depending on the measure of the system under study. Also, swarming strategies in bird flocking and fish schooling are utilized in the PSO and offered in [22]. However, PSO pains from the partial optimism, which produces the less exact at the regulation of its speed and the direction. Furthermore, the algorithm cannot work out the problems of scattering and optimization [23-24]. Moreover, the algorithm suffers from slow convergence in refined search stage, low local search ability and algorithm may lead to possible entrapment in local minimum solutions. A newer evolutionary computation algorithm, called BF scheme has been presented by [25-27] and further established by [28-29]. The BF algorithm depends on random search directions which may lead to protract in finding the global solution. A novel algorithm BF oriented by PSO is evolved that combine the above mentioned optimization algorithms [30-31]. This combination pursues to make use of PSO capability to exchange social information and BF ability in detecting a new solution by elimination and dispersal. This new hybrid technique called Bacterial Swarm Optimization (BSO) is used in this study to resolve the above aforesaid problems and drawbacks.

In this study, a comprehensive evaluation of the effects of the PSSs and SVC based control when independently applied and also via coordinated application has been performed. The design task of PSS and SVC based controller to evolve power system stability is transformed into an optimization task. The design objective is to enhance the stability of a multimachine power system, subjected to a disturbance. BSO technique is used to find the optimal PSS and SVC controller elements. BSO based SVC controller (BSOSVC) and BSO based PSS (BSOPSS) are discussed and their performances are compared with the coordinated design of BSOPSS and BSOSVC. Simulation results are introduced to ensure the robustness of the suggested controller to develop the power system dynamic stability. Also, a statistical T test is proceed to support the robustness of coordinated controller against uncoordinated one.

2. Problem Statement

A. Power System Model

A power system can be stated by a set of nonlinear differential equations as:

$$\dot{X} = f(X, U) \quad (1)$$

Where X is the vector of the state variables and U is the vector of input variables. In this study

$X = [\delta, \omega, E'_q, E_{fd}, V_f]^T$ and U is the PSS and SVC output signals. Here, δ and ω are the rotor angle and speed, respectively. Also, E'_q, E_{fd} and V_f are the internal, the field, and excitation voltages respectively.

In the planning of PSS and SVC, the linearized models around a balance point are used. Therefore, the state equation of a power system with n generators and m PSS and SVC can be stated as:

$$\dot{X} = AX + Bu \quad (2)$$

Where A is a $5n \times 5n$ matrix and equalizes $\partial f / \partial X$ while B is a $5n \times m$ matrix and equals $\partial f / \partial U$.

Both A and B are estimated at a certain operating point. X is a $5n \times 1$ state vector and U is an $m \times 1$ input vector.

B. PSS Modelling and Damping Controller Design

The operating task of a PSS is to create an appropriate torque on the rotor of the generator involved in such a way that the phase lag among the exciter and the generator electrical torque is compensated. The extra stabilizing signal is proportional to speed [32]. The block diagram of the i^{th} PSS with exciter is shown in Fig. 1.

Where $\Delta\omega_i$ is the deviation in speed from the synchronous speed. This kind of stabilizer composes of a washout filter, a dynamic compensator. The output signal is fed as an extra input signal, U_i to the regulator of the excitation system. The washout filter is applied to reset the steady state offset in the output of the PSS. The value of the time constant T_W is usually not critical and it may range from 0.5 to 20 s. The dynamic compensator is composed of two lead lag circuits and an extra gain. The adaptable PSS elements are the gain of the PSS, K_i and the time constants, $T_{li} - T_{4i}$. The lead lag block in the system reserves phase lead compensation for the phase lag

that is presented in the circuit between the exciter input and the electrical torque. The desired phase lead can be derived from the lead lag circuit even if the denominator portion composing of T_{2i} and T_{4i} allows a fixed lag angle.

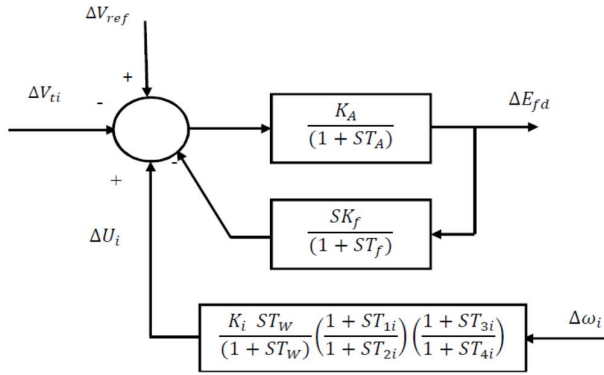


Fig. 1. Block diagram of i^{th} PSS with exciter.

C. SVC Modelling and Damping Controller Design

The thyristor controlled reactor in parallel with a fixed capacitor bank given in Fig. 2, is utilized in this work to develop the SVC model. Then, the system is shunt connected to the AC system via a set up transformer to get the voltages up to the desired transmission levels [8].

It is clear from (3) and Fig. 3, if the firing angle α of the thyristors is planned; SVC is capable to control the bus voltage magnitude. Time constant (T_r) and gain (K_r) represent the thyristors firing control system. The SVC parameters are presented in Appendix.

$$\dot{B}_e = \frac{1}{T_r} \left[-B_e + K_r (V_{ref} - V_t + V_s) \right] \quad (3)$$

The variable effective susceptance of the TCR is given by

$$B_V = -\frac{(2\pi - 2\alpha + \sin 2\alpha)}{\pi X_L} \quad \pi/2 \leq \alpha \leq \pi \quad (4)$$

Where X_L is the reactance of the fixed inductor of SVC. The effective reactance is

$$X_e = X_C \frac{\pi / r_x}{\sin 2\alpha - 2\alpha + \pi(2 - 1/r_x)} \quad (5)$$

Where $X_e = -1/B_e$ and $r_x = X_e / X_L$.

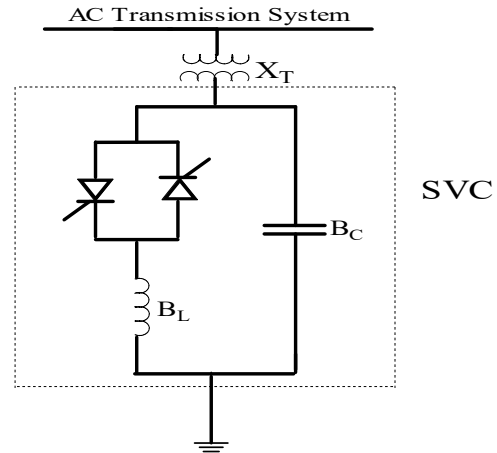


Fig. 2. SVC equivalent circuit.

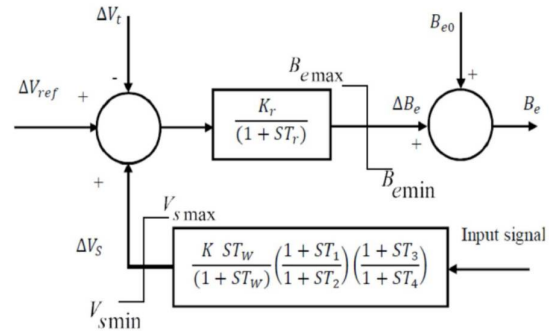


Fig. 3. Block diagram of SVC.

An extra stabilizing signal from speed can be required on the SVC control loop. The block diagram of a SVC with extra stabilizing signal is displayed in Fig. 3. This controller may be seen as a lead lag compensator. It includes gain block, limiter, signal washout circuit and two phases of lead lag compensator. The elements of the damping controllers for the aim of simultaneous coordinated design are gained using the BSO algorithm.

D. System under Study and SVC Location

Fig. 4 displays the single diagram of the used system. Details of system data are given in [33]. The participation matrix can be utilized in mode identity. Table (1) indicates the eigenvalues, and frequencies of the rotor modes. Examining Table (1) shows that the 0.2371 Hz mode is the interarea mode with G1 swinging versus G2 and G3. The 1.2955 Hz mode is the intermachine oscillation local to G2. Moreover, the 1.8493 Hz mode is the intermachine mode local

to G3. The positive real part of eigenvalue of G1 points instability of the system. The loading levels are shown in Table (2).

To determine the convenient placement of the SVC in the system, two designing will be given below. The first one is based on studying the impact of loading percentage while the second is interested with the line outage on voltages [34]. Tables (3, 4) show the effect of loading and line outage on node voltages of the system. It can be observed that the voltages are significantly affected at buses 5, and 6 respectively which are load buses. The reasons that rise the considerable voltage change are the relation of these buses with the longest lines in the system which has larger resistances and reactances than the others. Thus, the option of buses number 5 or 6 for installing the SVC controller is predicted to be the most compatible choice. Because both of them are near to generator number 1 which causes the system insecurity due to its unstable mode. Also, bus number 5 is the worst bus and will be taken as the best position for composing the SVC controller in this paper,[35]. Specially, the effect are presented in Table (3) and Table (4).

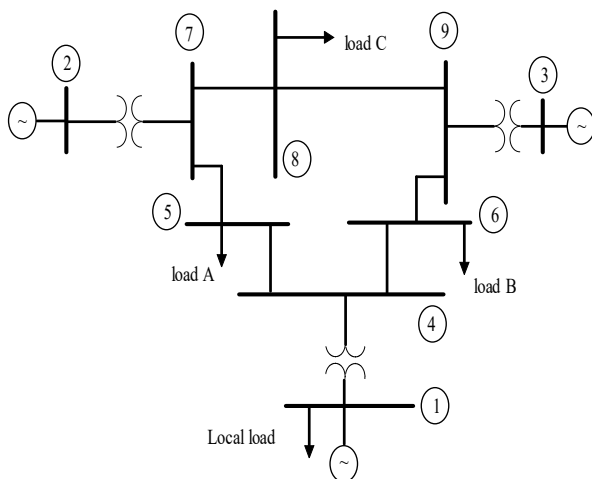


Fig. 4. System under study.

Table (1) The eigenvalues, and frequencies of the rotor modes.

Generator	Eigenvalues	Frequencies	Damping ratio ζ
G1	$+0.15 \pm 1.49j$	0.2371	-0.1002
G2	$-0.35 \pm 8.14j$	1.2295	0.0430
G3	$-0.67 \pm 11.62j$	1.8493	0.0576

Table (2) Loading of the system (in p.u)

	Light		Normal case		Heavy	
Generator	P	Q	P	Q	P	Q
G1	0.965	0.22	1.716	0.6205	3.57	1.81
G2	1.0	-0.193	1.63	0.0665	2.2	0.713
G3	0.45	-0.267	0.85	-1.086	1.35	0.43
Load	P	Q	P	Q	P	Q
A	0.7	0.35	1.25	0.5	2.0	0.9
B	0.5	0.3	0.9	0.3	1.8	0.6
C	0.6	0.2	1.00	0.35	1.6	0.65
at G1	0.6	0.2	1.00	0.35	1.6	0.65

Table (3) Effect of load percentage on load bus voltages

% Load	.25	.5	.75	1	1.25	1.5	1.75
Bus 4	1.06	1.05	1.04	1.03	1.01	0.99	0.98
Bus 5	1.06	1.04	1.02	0.99	0.96	0.94	0.9
Bus 6	1.06	1.05	1.03	1.01	0.99	0.97	0.94
Bus 7	1.05	1.04	1.04	1.03	1.01	1.00	0.98
Bus 8	1.05	1.04	1.03	1.02	0.99	0.98	0.96
Bus 9	1.05	1.05	1.04	1.03	1.02	1.01	1.0

Table (4) Effect of line outage on load bus voltages

line	4-5	4-6	5-7	6-9	7-8	8-9
Bus 4	1.039	1.028	0.996	1.005	1.016	1.022
Bus 5	0.839	0.998	0.938	0.968	0.974	0.989
Bus 6	1.020	0.942	0.975	0.964	0.999	1.009
Bus 7	0.988	1.022	1.017	1.016	1.019	1.010
Bus 8	0.989	1.006	1.001	1.005	0.969	0.978
Bus 9	1.024	1.017	1.019	1.023	1.013	1.034

3. Objective function

The elements of the PSSs and SVC can be elected to diminish the following objective function:

$$J = \int_0^{\infty} t \left(|\Delta w_{12}| + |\Delta w_{23}| + |\Delta w_{13}| \right) dt \quad (6)$$

Where $\Delta w_{12} = \Delta w_1 - \Delta w_2$, $\Delta w_{23} = \Delta w_2 - \Delta w_3$, and $\Delta w_{13} = \Delta w_1 - \Delta w_3$.

This index is relied on the Integral of Time multiple Absolute Error (ITAE). The merit of this elected performance indicator is that minimal dynamic plant information is required. To diminish the computational load in this work, the value of the wash out time constant T_W is specified to 10 second, the amounts of T_{2i} and T_{4i} are kept fixed at a sensible value of 0.05 second and setting of T_{1i} and T_{3i} are undertaken to acquire the net phase lead required by the system. Based on the objective function J optimization task can be modelled as: reduce J subjected to:

$$\begin{aligned} K_i^{\min} &\leq K_i \leq K_i^{\max} \\ T_{li}^{\min} &\leq T_{li} \leq T_{li}^{\max} \\ T_{3i}^{\min} &\leq T_{3i} \leq T_{3i}^{\max} \end{aligned} \quad (7)$$

Typical ranges of the optimized values are [1- 100] for K_i and [0.06-1.0] for T_{li} and T_{3i} .

This work focuses on coordinated plan of PSSs and SVC using BSO algorithm. The target of the optimization is to find for the optimum controller parameters setting that improve the damping characteristics of the system. Also, all controllers are planned simultaneously, taking into account the interaction among them.

4. Hybrid BF-PSO Optimization Algorithm

PSO is a stochastic optimization technique that draws inspiration from the behaviour of a flock of birds or a group of social insects with limited individual capabilities. In PSO a population of particles is initialized with random positions \vec{X}_i and

velocities \vec{V}_i , and a fitness function using the particle's positional coordinates as input values. Positions and velocities are detected, and the function is evaluated with the new coordinates at each time step [22-23]. The velocity and position equations for the d-th dimension of the i-th particle in the swarm may be stated as follows:

$$\begin{aligned} V_{id}(t+1) &= \omega V_{id}(t) + C_1 \phi_1 (X_{lid} - X_{id}(t)) + \\ &C_2 \phi_2 (X_{gd} - X_{id}(t)) \end{aligned} \quad (8)$$

$$X_{id}(t+1) = X_{id}(t) + V_{id}(t+1) \quad (9)$$

Where X_{lid} is the best position of every bacterial and X_{gd} is the global best bacterial.

Furthermore, the BF is based upon search and optimum foraging decision making abilities of the Escherichia coli bacteria [30]. The coordinates of a bacterium represent an individual solution of the optimization problem. Such a set of trial solutions converges towards the optimum solution following the foraging group dynamics of the bacteria population. Chemotactic movement is remained until a bacterium goes in the direction of positive nutrient gradient. After a certain number of complete swims the best half of the population undergoes reproduction, eliminating the rest of the population.

To escape local optima, an elimination dispersion event is performed where, some bacteria are liquidated at random with a small probability and the novel replacements are launched at random positions of the search space. A detailed description of the algorithm can be traced in [30-31]. Moreover, the flow chart of BSO is given in Fig. 5.

[Step 1] Initialize parameters n, S, N_C, N_S, N_{re} ,

$N_{ed}, P_{ed}, C(i)(i=1,2,\dots,N), \phi^i$.

Where,

n : Dimension of the search space,

S : The number of bacteria in population,

N_{re} : The number of reproduction steps,

N_C : The number of chemotactic steps,

N_S : Swimming length after which tumbling of bacteria is performed in a chemotaxis loop,

N_{ed} : The number of elimination-dispersal events to be imposed over the bacteria,

P_{ed} : The probability with which the elimination and dispersal will continue,

$C(i)$: The size of the step taken in the random direction specified by the tumble,

ω : The inertia weight,

C_1, C_2 : The swarm confidence,

$\vec{\theta}(i, j, k)$: Position vector of the i-th bacterium, in j-th chemotactic step and k-th reproduction,

\vec{V}_i : Velocity vector of the i-th bacterium.

[Step 2] Update the following

$J(i, j, k)$: Cost or fitness value of the i-th bacterium in the j-th chemotaxis, and the k-th reproduction loop.

$\vec{\theta}_{g_best}$: Position vector of the best position found by all bacteria.

$J_{best}(i, j, k)$: Fitness value of the best position found so far.

[Step 3] Reproduction loop: $k = k + 1$

[Step 4] Chemotaxis loop: $j = j + 1$

[Sub step a] For $i=1, 2, \dots, S$, take a chemotaxis step for bacterium i as follows.

[Sub step b] Compute fitness function, $J(i, j, k)$.

[Sub step c] Let $J_{last} = J(i, j, k)$ to save this value since one may find a better cost via a run.

[Sub step d] Tumble: generate a random vector

$\Delta(i) \in R^n$ with each element

$\Delta_m(i), m = 1, 2, \dots, n$, a random number on $[-1, 1]$

[Sub step e] Move: Let

$$\theta(i, j+1, k) = \theta(i, j, k) + C(i) \frac{\Delta(i)}{\sqrt{\Delta^T(i)\Delta(i)}}$$

[Sub step f] Compute $J(i, j+1, k)$.

[Sub step g] Swim: one considers only the i -th bacterium is swimming while the others are not moving then

i) Let $m=0$ (counter for swim length).

ii) While $m < N_s$ (have not climbed down too long)

• Let $m = m + 1$

• If $J(i, j+1, k) < J_{last}$ (if doing better),

Let $J_{last} = J(i, j+1, k)$ and let

$$\theta(i, j+1, k) = \theta(i, j, k) + C(i) \frac{\Delta(i)}{\sqrt{\Delta^T(i)\Delta(i)}}$$

use this $\theta(i, j+1, k)$ to compute the new

$J(i, j+1, k)$ as shown in new [sub step f]

• Else, let $m = N_s$. This is the end of the while statement.

[Step 5] Mutation with PSO operator

For $i=1, 2, \dots, S$

• Update the $\vec{\theta}_{g_best}$ and $J_{best}(i, j, k)$

• Update the position and velocity of the d -th coordinate of the i -th bacterium according to the following rule:

$$V_{id}^{new} = \omega V_{id}^{new} + C_1 \phi_1 \left(\theta_{g_best_d} - \theta_d^{old}(i, j+1, k) \right)$$

$$\theta_d^{new}(i, j+1, k) = \theta_d^{old}(i, j+1, k) + V_{id}^{new}$$

[Step 6] Let $S_r = S/2$

The S_r bacteria with highest cost function (J) values die and other half bacteria population with the best values split.

[Step 7] If $k < N_{re}$, go to [step 3]. One has not reached the number of specified reproduction steps, so one starts the next generation in the chemotaxis loop.

More details of BF and PSO parameters are presented in Appendix.

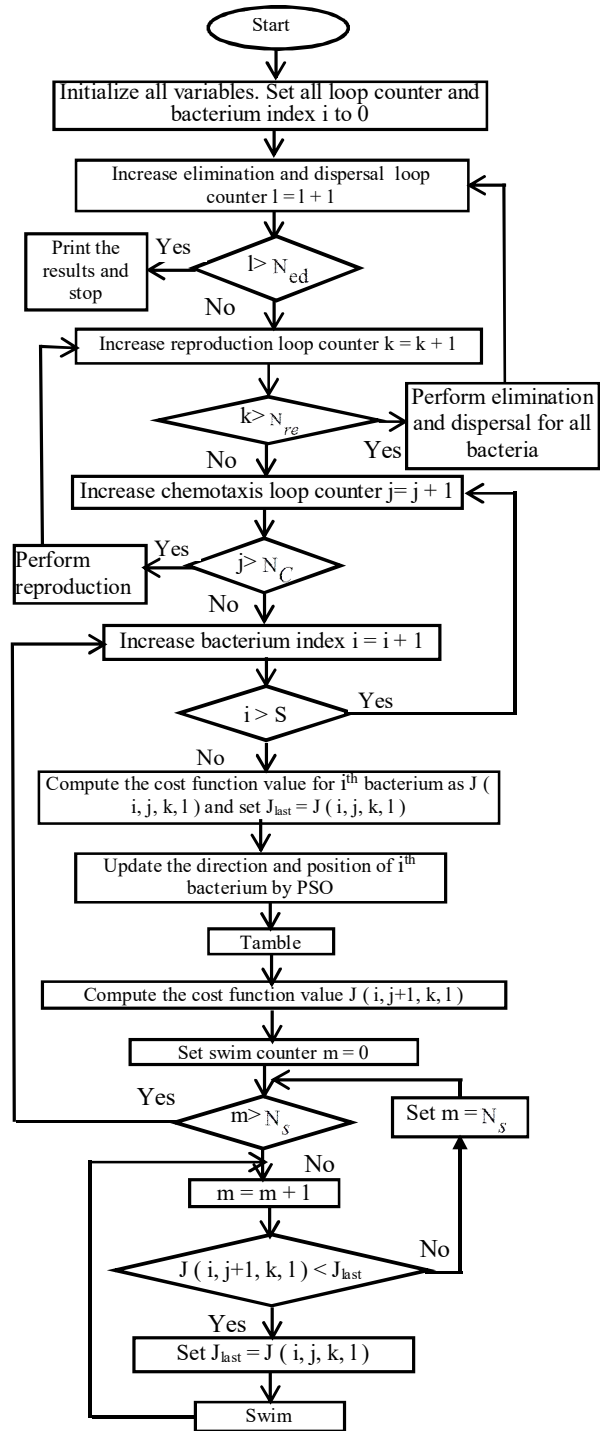


Fig. 5. Flow chart of BSO algorithm.

5. Results and Simulations

Fig. 6. shows the change of objective function with various techniques. The algorithm is run keeping limiting value of cost function at 10^{-6} . It was found that the BSO gives faster convergence than PSO and

BF. Furthermore, BSO converges at a faster rate (44 iterations) compared with that for PSO (68 iterations) and BFOA (88 iterations). Also, computational time (CPU) of both algorithms is compared based on the average CPU time taken to converge the solution. The average CPU for BSO is 43.4 second while it is 68.3 and 79.2 second for PSO and BF respectively.

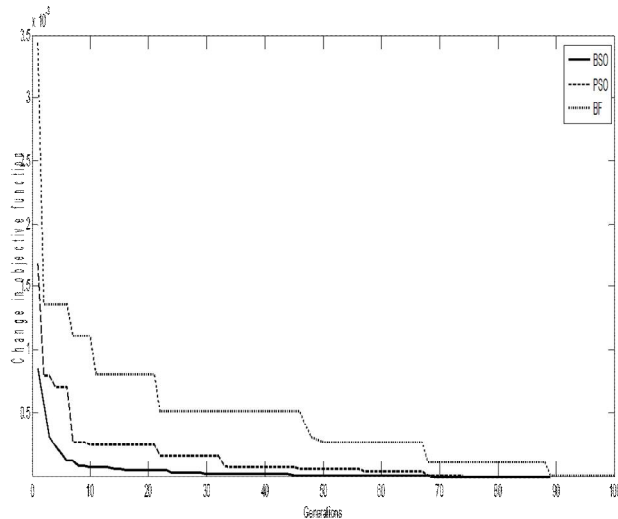


Fig. 6. Change in objective function.

Table (5), gives the system eigenvalues, and damping ratio of mechanical mode with several loading conditions. It is clear that, the system with BSOSVC has small damping factors ($\sigma = -0.65, -0.69, -1.06$) for light, normal, and heavy loading respectively. Also, the suggested coordinated controller shifts substantially the electromechanical eigenvalues to the left of the S-plane and the values of the damping factors with the suggested coordinated controller are improved significantly to be ($\sigma = -1.13, -1.17, -1.57$) for light, normal, and heavy loading respectively. Moreover, the damping ratios corresponding to coordinated controller are better than that corresponding to individual ones. Thus, compared with the BSOSVC and BSOPSS, the suggested coordinated controller greatly improves the system stability and enhances the damping behaviour of electromechanical modes. Results of various controllers parameters set values based on the time domain objective function using BF are displayed in Table (6).

Table (5) Mechanical modes and ζ under various loading.

	BSOSVC	BSOPSS	Coordinated	Uncoordinated
Light load	$-3.1 \pm 9.87j$	$-3.76 \pm 6.1j$	$-4.74 \pm 7.39j$	$-3.32 \pm 9.42j$
	0.2997	0.5247	0.54	0.3324
	$-3.83 \pm 7.45j$	$-4.88 \pm 6.37j$	$-4.98 \pm 6.09j$	$-1.13 \pm 6.72j$
	0.4572	0.6081	0.633	0.1658
	$-0.65 \pm 0.79j$	$-0.97 \pm 0.67j$	$-1.13 \pm 0.72j$	$-0.44 \pm 0.75j$
Normal load	0.6354	0.8228	0.8434	0.50
	$-3.27 \pm 11.3j$	$-3.95 \pm 8.29j$	$-3.98 \pm 8.14j$	$-3.01 \pm 8.85j$
	0.277	0.4301	0.4392	0.322
	$-2.76 \pm 9.0j$	$-4.24 \pm 6.32j$	$-4.51 \pm 6.34j$	$-1.21 \pm 6.63j$
	0.2932	0.5571	0.5797	0.1795
Heavy load	$-0.69 \pm 0.78j$	$-0.95 \pm 0.74j$	$-1.17 \pm 0.63j$	$-0.38 \pm 0.74j$
	0.6626	0.7889	0.8805	0.4568
	$-2.9 \pm 11.38j$	$-3.67 \pm 8.42j$	$-3.93 \pm 8.27j$	$-3.04 \pm 8.96j$
	0.2461	0.398	0.4292	0.3213
	$-1.97 \pm 8.78j$	$-3.97 \pm 6.55j$	$-4.13 \pm 5.9j$	$-1.24 \pm 6.76j$
	0.2189	0.5183	0.5735	0.1804
	$-1.06 \pm .83j$	$-1.08 \pm 0.83j$	$-1.57 \pm 0.73j$	$-0.45 \pm 0.87j$
	0.7873	0.7929	0.9068	0.4594

Table (6) Optimal PSSs and SVC parameters for different controllers.

	Coordinated Design				Uncoordinated Design			
	PSS1	PSS2	PSS3	SVC	PSS1	PSS2	PSS3	SVC
K	49.51	1.4931	1.7437	0.9158	31.24	8.4379	6.3887	63.721
T_1	0.4652	0.5827	0.3716	0.3712	0.6839	0.3462	0.2479	0.7423
T_3	0.2684	0.2119	0.1052	0.2882	0.5165	0.1385	0.3253	0.5978

A. Response under normal loading

Fig. 7 and Fig. 8, give the response for normal loading. The results of these studies show that the suggested coordinated controller has an excellent ability in damping power oscillations and greatly improves the dynamic stability of the system. Also, the settling times of oscillations are $T_s = 1.7, 2.0$, and 2.2 second for coordinated controller, BSOPSS, and BSOSVC respectively so the suggested controller is able of supplying enough damping to the system oscillatory modes. Thus, the coordinated controller extends the system stability limit and the power transfer ability.

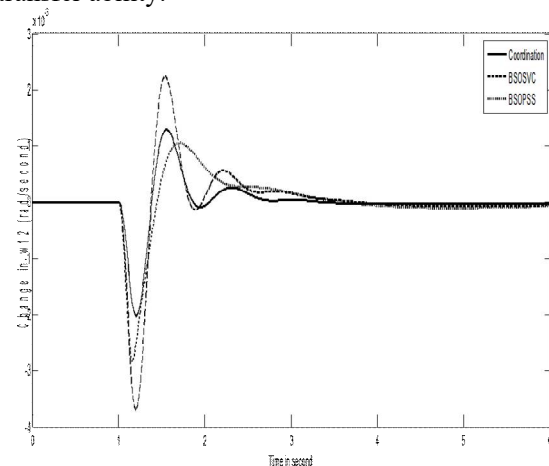


Fig. 7. Change of $\Delta\omega_{12}$ under normal loading.

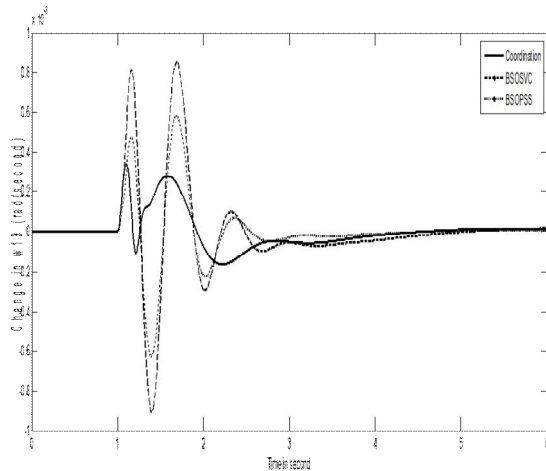


Fig. 8. Change of $\Delta\omega_{13}$ under normal loading.

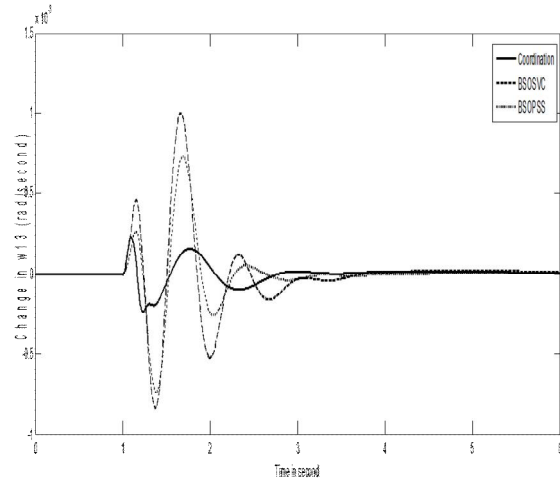


Fig. 10. Change of $\Delta\omega_{13}$ under heavy loading.

B. Response under heavy load condition

Fig. 9 and Fig. 10, show the system response at heavy loading with fixing the controllers parameters. It can be seen that the response with the suggested coordinated controller gives good damping behaviour to low frequency oscillations and the system is more quickly stabilized than BSOPSS and BSOSVC. Also, the settling times of these oscillations are $T_s=1.7, 2.0$, and 2.2 second for coordinated controller, BSOPSS, and BSOSVC respectively. Thus, the simulations results reveal that the simultaneous coordinated planning of the BSOSVC damping controller and the BSOPSS explains its notability to both the uncoordinated designed controller of the BSOSVC and the BSOPSS. Moreover, this controller has a soft architecture and the potentiality of application in real time environment.

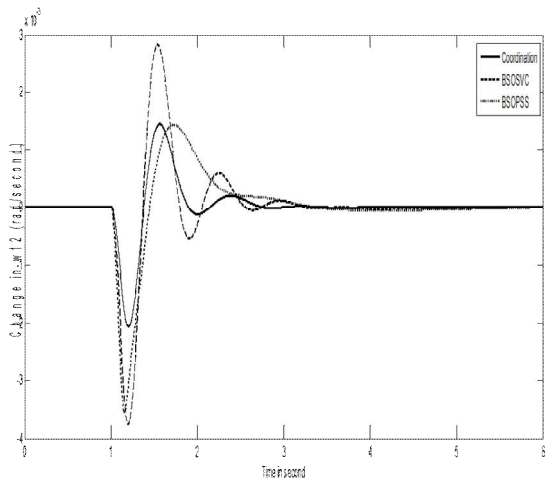


Fig. 9. Change of $\Delta\omega_{12}$ under heavy loading.

C. Statistical T test

To assess the robustness of the suggested coordinated controller, the performance of the system with the suggested coordinated controller is compared to uncoordinated one. A statistical T test is performed between the coordinated controller and uncoordinated one to assess the robustness of the suggested coordinated controller. The damping ratios of mechanical modes for the coordinated and uncoordinated controller under various loading conditions are elected as input to statistical T test. This test determines that, is there a specific different between two controllers or not?

Let the null hypothesis: $H_0 = \mu_1 - \mu_2 = 0$

Let the alternative hypothesis: $H_1 = \mu_1 - \mu_2 > 0$

Where μ_1, μ_2 are the mean values of damping ratios of coordinated and uncoordinated controller respectively. The significance level $\alpha = 0.05$ is established. Table (7) gives the output parameters of the statistical T test. The input to the T test is the damping ratios of the rotor modes for various controllers and operating conditions. The result concludes to reject H_0 . Moreover, one can decide from this test that there is a respectable moral difference between the two controllers. Also, the output of $\Delta\omega_{12}$ for coordinated and uncoordinated controller is indicated in Fig. 11. This Figure shows the superiority of the suggested coordinated controller in decreasing the settling time and damping power oscillations versus uncoordinated one.

Table (7) Output parameters of statistics T-test.

t-Test: Paired Two Sample for Means		
	Coordinated	Uncoordinated
Mean	0.647255556	0.324177778
Variance	0.03409811	0.016694377
Observations	9	9
Pearson Correlation	0.646251843	
Hypothesized Mean Difference	0	
df	8	
t Stat	6.861275353	
P(T<=t) one-tail	6.47503E-05	
t Critical one-tail	1.859548033	
P(T<=t) two-tail	0.000129501	
t Critical two-tail	2.306004133	

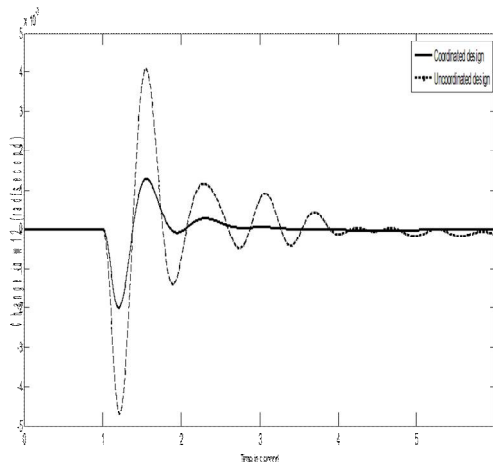


Fig. 11. Comparison between coordinated and uncoordinated design.

6. Conclusions

The statistical evaluation of the robust coordinated design of PSSs and SVC damping controller in a power system is proposed in this paper. The design task of the suggested controller is established as an optimization process and BSO is used to search for optimal controller parameters. Simulations results assure the robustness of the suggested coordinated controller in supplying good damping characteristic to system oscillations for a wide range of loading conditions and large disturbance. Also, it is supreme to uncoordinated controller through the statistical evaluation. Coordination between various devices via fresh optimization algorithms is the future work of this paper.

7. References

[1] P. Kundur, "Power System Stability and Control", McGraw-Hill, 1994.

[2] Y. S. Lee, and S. Y. Sun, "STATCOM Controller Design for Power System Stabilization with Sub-optimal Control and Strip Pole Assignment", Int. J. of Electrical Power and Energy Systems, Vol. 24, No. 9, November 2002, pp. 771-779.

[3] M. A. Abido, "Optimal Design of Power System Stabilizers using Particle Swarm Optimization" IEEE Transactions on Energy Conversion, Vol. 17, No. 3, September 2002, pp. 406-413.

[4] Y.L. Abdel-Magid, and M.A. Abido, "Coordinated Design of a PSS and a SVC Based Controller to Enhance Power System Stability", Int. J. of Electrical Power and Energy Systems, Vol. 25, No. 9, November 2003, pp. 695-704.

[5] J. Baskaran, and V. Palanisamy, "Optimal Location of FACTS Devices in a Power System Solved by a Hybrid Approach", Int. J. of Nonlinear Analysis, Vol. 65, No. 11, December 2006, pp. 2094-2102.

[6] S. Kodsi, C. Canizares, and M. Kazerani, "Reactive Current Control Through SVC for Load Power Factor Correction", Int. J. of Electric Power Systems Research, Vol. 76, No. 9-10, June 2006, pp. 701-708.

[7] S. A. Al-Baiyat, "Design of a Robust SVC Damping Controller Using Nonlinear H_{∞} Technique", The Arabian Journal for Science and Engineering, Vol. 30, No. 1B, April 2005, pp. 65-80.

[8] K. Ellithy, and A. Al-Naamany, "A Hybrid Neuro-Fuzzy Static Var Compensator Stabilizer for Power System Damping Improvement in the Presence of Load Parameters Uncertainty", Int. J. of Electric Power Systems Research, Vol. 56, No. 3, December 2000, pp. 211-223.

[9] P. K. Modi, S. P. Singh, and J. D. Sharma, "Fuzzy Neural Network Based Voltage Stability Evaluation of Power Systems with SVC", Applied Soft Computing, Vol. 8, No. 1, January 2008, pp. 657-665.

[10] M. H. Haque, "Best Location of SVC to Improve First Swing Stability of a Power System", Int. J. of Electric Power System Research, Vol. 77, No. 10, August 2007, pp. 1402-1409.

[11] Y. Chang, and Z. Xu, "A Novel SVC Supplementary Controller Based on Wide Area Signals", Int. J. of Electric Power System Research, Vol. 77, No. 12, August 2007, pp. 1569-1574.

[12] S. Panda, N. P. Patidar, and R. Singh, "Simultaneous Tuning of SVC and Power System Stabilizer Employing Real-Coded Genetic Algorithm", Int. J. of Electrical and Electronics Engineering, Vol. 4, No. 4, 2009, pp. 240-247.

- [13] C. Rakpenthai, S. Premrudeepreechacharn, and S. Uatrangjit, "Power System with Multi-Type FACTS Devices States Estimation Based on Predictor-Corrector Interior Point Algorithm", Int. J. of Electrical Power and Energy Systems, Vol. 31, No. 4, May 2009, pp. 160–166.
- [14] E. Zhijun, D. Z. Fang, K. W. Chan, and S. Q. Yuan, "Hybrid Simulation of Power Systems with SVC Dynamic Phasor Model", Int. J. of Electrical Power and Energy Systems, Vol. 31, No. 5, June 2009, pp. 175–180.
- [15] Y. Yuan, G. Li, L. Cheng, Y. Sun, J. Zhang, and P. Wang, "A Phase Compensator for SVC Supplementary Control to Eliminate Time Delay by Wide Area Signal Input", Int. J. of Electrical Power and Energy Systems, Vol. 32, No. 3, March 2010, pp. 163–169.
- [16] E. S. Ali, "Static Var Compensator Design for Power System Stabilization Using Bacteria Foraging Optimization Algorithm", 13th International Middle East Power Systems Conference (MEPCON 2009), Assiut University, Assiut, Egypt, December 20–23, 2009, pp. 578–582.
- [17] A. Y. Abd-Elaziz, and E. S. Ali, "Static VAR Compensator Damping Controller Design Based on Flower Pollination Algorithm for a Multi-machine Power System", Electric Power Components and System, Vol. 43, Issue 11, 2015, pp. 1268–1277.
- [18] X. Y. Bian, C. T. Tse, J. F. Zhang, and K. W. Wang, "Coordinated Design of Probabilistic PSS and SVC Damping Controllers", Int. J. of Electrical Power and Energy Systems, Vol. 33, No. 3, March 2011, pp. 445–452.
- [19] M. A. Furini, A. L. S. Pereira, and P. B. Araujo, "Pole Placement by Coordinated Tuning of Power System Stabilizers and FACTS POD Stabilizers", Int. J. of Electrical Power and Energy Systems, Vol. 33, No. 3, March 2011, pp. 615–622.
- [20] S. Panda, "Multi-objective PID Controller Tuning for a FACTS Based Damping Stabilizer Using Non-dominated Sorting Genetic Algorithm-IP", Int. J. of Electrical Power and Energy Systems, Vol. 33, No. 7, September 2011, pp. 1296–1308.
- [21] S. M. Abd-Elazim, and E. S. Ali, "Synergy of Particle Swarm Optimization and Bacterial Foraging for TCSC Damping Controller Design", Int. J. of WSEAS Transactions on Power Systems, Vol. 8, No. 2, April 2013, pp. 74–84.
- [22] J. Kennedy and R. Eberhart, "Particle Swarm Optimization", Proceedings of IEEE International Conference on Neural Networks, 1995, pp. 1942–1948.
- [23] D. P. Rini, S. M. Shamsuddin, and S. S. Yuhani, "Particle Swarm Optimization: Technique, System and Challenges", Int. J. of Computer Applications, Vol. 14, No. 1, January 2011, pp. 19–27.
- [24] V. Selvi and R. Umarani, "Comparative Analysis of Ant Colony and Particle Swarm Optimization Techniques", Int. J. of Computer Applications, Vol. 5, No. 4, August 2010, pp. 1–6.
- [25] K. M. Passino, "Biomimicry of Bacterial Foraging for Distributed Optimization and Control", IEEE Control System Magazine, Vol. 22, No. 3, June 2002, pp. 52–67.
- [26] S. Mishra, "A Hybrid Least Square Fuzzy Bacteria Foraging Strategy for Harmonic Estimation", IEEE Trans. Evolutionary Computer, Vol. 9, No.1, February 2005, pp. 61–73.
- [27] D. B. Fogel, "Evolutionary Computation towards a New Philosophy of Machine Intelligence", IEEE, New York, 1995.
- [28] E. S. Ali, S. M. Abd-Elazim, "Optimal PSS Design in a Multimachine Power System via Bacteria Foraging Optimization Algorithm", Int. J. of WSEAS Transactions on Power Systems, Vol. 8, No. 4, October 2013, pp. 186–196.
- [29] E. S. Ali, S. M. Abd-Elazim, "Hybrid BFOA-PSO Approach for Optimal Design of SSSC Based Controller", Int. J. of WSEAS Transactions on Power Systems, Vol. 9, No. 1, January 2014, pp. 54–66.
- [30] A. Biswas, S. Dasgupta, S. Das, and A. Abraham, "Synergy of PSO and Bacterial Foraging Optimization: A Comparative Study on Numerical Benchmarks", Innovations in Hybrid Intelligent Systems, ASC 44, 2007, pp. 255–263.
- [31] W. Korani, "Bacterial Foraging Oriented by Particle Swarm Optimization Strategy for PID Tuning", GECCO'08, July 12–16, 2008, Atlanta, Georgia, USA, pp. 1823–1826.
- [32] P. Kundur, M. Klein, G. J. Rogers, and M. S. Zywno, "Application of Power System Stabilizers for Enhancement of Overall System Stability", IEEE Trans. Power System, Vol. 4, No. 2, 1989, pp. 614–626.
- [33] P. M. Anderson and A. A. Fouad, "Power System Control and Stability", Iowa State University Press, Iowa, 1977.
- [34] S. M. Abd-Elazim, "Comparison between SVC and TCSC Compensators on Power System Performance", Master thesis, 2006, Zagazig University, Egypt.

- [35] S. M. Abd-Elazim, and E. S. Ali, “A Hybrid Particle Swarm Optimization and Bacterial Foraging for Power System Stability Enhancement”, IEEE, 15th International Middle East Power Systems Conference “MEPCON’12”, Alexandria University, Egypt, December 23-25, 2012.

Appendix

The system data are as shown below:

- a) Excitation system: $K_A = 400$; $T_A = 0.05$ second; $K_f = 0.025$; $T_f = 1$ second.
- b) SVC Controller: $T_r = 15$ msecod; $\alpha_0 = 140$; $K_r = 50$.
- c) Bacteria parameters: Number of bacteria =10; number of chemotactic steps =10; number of elimination and dispersal events = 2; number of reproduction steps = 4; probability of elimination and dispersal = 0.25; the values of $d_{attract} = 0.01$; the values of $\omega_{attract} = 0.04$; the values of $h_{repellent} = 0.01$; the values of $\omega_{repellent} = 10$.
- d) PSO parameters: $C_1 = C_2 = 2.0$, $\omega = 0.9$.

Conflicts of Interest

The author(s) declare no potential conflicts of interest concerning the research, authorship, or publication of this article.

Contribution of individual authors to the creation of a scientific article (ghostwriting policy)

The author(s) contributed in the present research, at all stages from the formulation of the problem to the final findings and solution.

Sources of funding for research presented in a scientific article or scientific article itself

No funding was received for conducting this study.

Creative Commons Attribution License 4.0 (Attribution 4.0 International, CC BY 4.0)

This article is published under the terms of the Creative Commons Attribution License 4.0 https://creativecommons.org/licenses/by/4.0/deed.en_US